Modelling of strain rate effects on matrix dominated elastic and failure properties of unidirectional fibre-reinforced polymer-matrix composites

L Raimondo[a,1], L Iannucci[a], P Robinson[a], and PT Curtis[b]

[a] Imperial College London, South Kensington Campus, SW7 2AZ London, UK

[b] Physical Sciences Department, DSTL, 415 BLDG, Porton Down, SP4 0JQ Wiltshire, UK

Abstract

A phenomenological-based, strain rate dependent failure theory, which is suitable for the numerical modelling of unidirectional (UD) carbon fibre reinforced polymer composites (CFRP), is presented. A phenomenological-based approach is also proposed for the three-dimensional (3D) modelling of strain rate induced material hardening in UD polymer composites. The proposed theory and approach are implemented in the Finite Element (FE) code ABAQUS/Explicit for one integration point solid elements. Validation is presented against experimental data from dynamic compressive tests using results available in the published literature.

Conclusions indicate that the proposed method can be applied for predicting the elastic and failure properties of UD carbon fibre polymer composites for generic, 3D, quasi-static (QS) and high-rate loading conditions with very good accuracy. In particular, it is shown that the phenomenological approach to modelling here proposed allows prediction of all matrix dominated properties, i.e. moduli of elasticity and strength, including parallel-to-the fibres compression strength, with the knowledge of one strain rate dependent parameter, which is characterised using dynamic strength data for one specimen configuration.

Key-words: A. Carbon fibres; B. Polymer-matrix composites (PMCs); B. Impact behaviour; B. Mechanical properties; C. Finite element analysis (FEA)

1. Introduction

Macro-mechanically based models have been developed to predict the 3D non-linear behaviour of polymer composites and these are founded on classic plasticity theories. One of the advantages of the models based on plasticity theories is that they can be easily extended for predicting strain rate effects, and can be implemented in FE for numerical analysis, e.g. [1], [2], [3]. These models typically require that parameters are defined from fitting of data from a full range of off-axis tests for predicting the composite's behaviour in the generic case. The applicability of classic visco-plastic models, when the 3D plastic potential is not characterised, is in fact limited to uni-axial loading conditions [2]. Visco-plasticity combined with micro-mechanics approaches have also been proposed, e.g. [4], [5]. These require that constituent elastic constants are determined from composite data using micromechanics, which is a limitation because it requires further computational effort.

[1] Corresponding author.
Tel: +44 (0)20 7594 5113
Fax: +44 (0)20 7594 1974
E-mail address: l.raimondo@imperial.ac.uk

Dynamic failure theories have also been proposed for UD composites, but they typically require high-rate tests data to be produced for many different specimen configurations [6].

The work described in the current paper is motivated by the need to surpass the above limitations. In order to achieve this, a constitutive modelling approach based on physically sound arguments should be preferred amongst the various available approaches. This is because phenomenological-based models have the potential to succeed in accurately simulating material behaviour in a loading space that extends beyond the space of characterisation of the material parameters requiring less fitting parameters to be determined from experiments.

The objective of the current paper is two-folds: 1) to propose a new set of dynamic failure criteria, which includes a new criterion for dynamic fibre compressive failure and new phenomenological-based, strain rate dependent criteria for matrix tensile and compressive failure; 2) to propose a strain rate dependent, phenomenological-based hardening model, which can be used alternatively to classic visco-plasticity in combination with the proposed dynamic failure criteria.

The proposed model can be applied to predicting strain-rate effects on matrix dominated elastic and failure properties of UD CFRP composites, and can be easily implemented into commercial FE software for explicit analysis. It is shown that its application, with numerical simulations, can dramatically reduce the characterisation effort and improve predictive capabilities when compared to other currently available approaches.

2. Dynamic failure criteria for UD carbon fibre polymer composites

2.1 Fibre tensile failure

Experimental failure envelopes for UD composites subject to bi-axial loadings make it too difficult to conclude whether stresses other than σ_x contribute to fibre failure. Thus, the maximum stress criterion is proposed here:

$$f_{ft} = \left(\frac{\sigma_x}{X_t} \right)^2 - 1 \geq 0 \qquad \text{Equation (1)}$$

Where X_t is the tensile strength of the composite in the fibre direction, which is identified with the index *x*. X_t is assumed equal to the QS value also at higher strain rates, which is supported by experimental evidence [1], [7], [8], [9].

2.2 Fibre compressive failure

Longitudinal compressive failure of UD composites is driven by shear mechanisms in a complex manner. A first crack may be started by shear fracture of the fibres, followed by rotation of the fibres and in-plane shearing of the matrix at the crack tip, which in turn promotes kink band development [10]. However, depending on the material, a kink band can also be promoted prior to fibre failure by an initial fibre misalignment [11]. Thus, compressive failure envelopes for combined compression/shear are strongly dependent on the material investigated, see Figure 1, which shows a selection of experimental results available in the literature [12], [13], [14].

Stress interactive failure criteria for composites have been developed from polynomials derived from stress tensor expansion, which is a technique originally proposed for failure analysis of metals [15], by including anisotropic strength parameters [16]. These classes of criteria, which can be also expressed in terms of the stress invariants [17], implicitly assume a perfectly aligned fibre arrangement. Phenomenological-based expressions have been proposed for predicting the pure longitudinal compressive failure strength from shear strength, and assume an initial fibre misalignment [18], [19], [20], [21]. In the latest and most advanced interactive criteria for fibre compressive failure [20], [21], the fibre-misalignment angle is required as an input material property, whose value may encompass anything from an actual fibre-misalignment to structural defects, oscillations in fibre volume fraction, matrix cracks etc. [21]. Thus, these criteria offer a good match with the experimental failure envelopes only when their calibration is carried out with some form of data-fitting. For reasons of simplicity, the criterion for fibre compressive failure is here derived directly from polynomial-based curve fitting of the experimental failure envelopes, i.e. for QS loading:

$$f_{fc} = \frac{\sigma_x}{X_c^{qs}} + \left(\frac{\tau_{xy}}{S_{xy}^{qs}}\right)^{\alpha} + \left(\frac{\tau_{zx}}{S_{zx}^{qs}}\right)^{\alpha} - 1 \geq 0 \qquad \text{Equation (2)}$$

Which, depending on the phenomenology of failure, offers a good fit for $\alpha \geq 1$, see Figure 1. When considering the shear nature of compressive failure mechanisms, it is not a surprise that most of the published data in the literature indicates that the longitudinal compressive strength of UD composites is greatly affected by strain rate [22], [23], [24], [25], [26], [27], [28].

Hsiao and Daniel [25] proposed a graphical determination of the longitudinal compressive QS strength X_c^{qs} based on the following relationship:

$$X_c^{qs} = \frac{\tau^*}{\vartheta + \gamma^*} \qquad \text{Equation (3)}$$

Where ϑ is the initial fibre misalignment, and τ^*, γ^* are values of shear stress and strain as defined in Figure 2, which shows a typical stress strain curve for a UD carbon/epoxy composite. It is evident that, based on this graphical interpretation, $\tau_{yield} < \tau^* < S_{xy}$, i.e. τ^* must be a value that is greater than the shear yield strength τ_{yield} and lower than the shear failure strength S_{xy}. Experimental evidence indicates that the shear yield strength increases more with strain rate than it does the shear failure strength, e.g. [29].

Thus, the dynamic longitudinal compressive strength X_c^d of a composite with an initial fibre misalignment is here conservatively defined as:

$$X_c^d = k_{xy}(\dot{\varepsilon}_x) X_c^{qs} \qquad \text{Equation (4)}$$

In which k is a scaling function for strength, derived from fitting the shear strength vs. strain rate data, i.e.:

$$k_{xy}(\dot{\gamma}_{xy}) = \frac{S_{xy}^d(\dot{\gamma}_{xy})}{S_{xy}^{qs}} \qquad \text{Equation (5)}$$

Equation (4) is formulated with the assumption that under longitudinal compression, the in-plane shear strain triggered by an initial fibre misalignment grows at a rate that has the same order of magnitude than the axial strain rate. The following criterion is thus proposed for predicting the compressive strength in the fibre direction, for QS and high-rate loading conditions:

$$f_{fc} = \frac{\sigma_x}{k_{xy}\left(\dot{\varepsilon}_x^t\right) X_c^{qs}} + \frac{\tau_{xy}}{k_{xy}\left(\dot{\gamma}_{xy}\right) S_{xy}^{qs}} + \frac{\tau_{zx}}{k_{xy}\left(\dot{\gamma}_{zx}\right) S_{zx}^{qs}} - 1 \geq 0 \qquad \text{Equation (6)}$$

Equation (6) is valid for transversely isotropic UD carbon/polymer composites with an initial fibre misalignment. For composites that fail as a result of shear failure of the fibres, the following criterion might be more suitable:

$$f_{fc} = \frac{\sigma_x}{X_c^{qs}} + \left(\frac{\tau_{xy}}{k_{xy}\left(\dot{\gamma}_{xy}\right) S_{xy}^{qs}} \right)^{\alpha} + \left(\frac{\tau_{zx}}{k_{zx}\left(\dot{\gamma}_{zx}\right) S_{zx}^{qs}} \right)^{\alpha} - 1 \geq 0 \qquad \text{Equation (7)}$$

There are no failure envelopes in the literature for combined longitudinal compression/in-plane shear dynamic loading of UD polymer composites. The extreme ends of the failure envelope are validated in this paragraph. The shear components are trivially validated because the $k_{ij}\left(\dot{\gamma}_{ij}\right)$ scaling functions are directly calibrated using dynamic and QS shear strength data, this will be explained in Section 2.6.

The normalised values of both longitudinal compressive strength and in-plane shear strength for various UD carbon/polymer composites are plotted versus strain rate in Figure 3. These values were taken from [30], in which experimental results from various works published in the literature were collated. Results in this Figure 3 imply the general validity of Equation (4).

Only two works have been published in which both the longitudinal compressive strength and the in-plane shear strength were characterised for a same material at QS and dynamic loading rates, i.e. [25], and [29] in combination with [28]. The experimental results published in both of these works confirm that Equation (4) predicts the longitudinal compressive strength of the UD composites investigated with remarkable accuracy and over a wide range of strain rates, i.e. between 10^{-4} and 10^{2} s^{-1}, see Table 1. Also, experimental off-axis compression tests results have been published in the literature, e.g. [29]. The validation against off-axis data requires numerical simulations, and it will be shown in Section 4.

2.3 Matrix tensile failure

Advanced phenomenological-based matrix failure criteria for 3D QS failure analysis of UD composites have been recently formulated by Pinho et al. [21] based on previous work by Puck [31], Puck and Schurmann [32] and by Davila et al. [20]. The latest matrix failure criteria form the basis of the research work presented in this and in the next Section 2.4. In these sections, the applicability of the tensile and compressive failure criteria proposed in [21] for QS loading conditions is extended to dynamic loading conditions.

The following criterion is proposed for matrix tensile dynamic failure:

$$\begin{cases} \left(\sigma_i\right) \xrightarrow{\perp x(\varphi)} \left(\sigma_{i'}\right) \\ \left(\dot{\varepsilon}_i\right) \xrightarrow{\perp x(\varphi)} \left(\dot{\varepsilon}_{i'}\right) \\ f_{mt} = \left(\dfrac{\sigma_{y'}}{Y_t^{qs}}\right)^2 + \left(\dfrac{\tau_{xy'}}{k_{xy'}\left(\dot{\gamma}_{xy'}\right)S_{xy}^{qs}}\right)^2 + \left(\dfrac{\tau_{y'z'}}{k_{y'z'}\left(\dot{\gamma}_{y'z'}\right)S_{yz}^{qs}}\right)^2 - 1 \geq 0 \end{cases} \quad \text{Equation (8)}$$

Where the symbol $\perp x(\varphi)$ signifies a 3D rotation around the x-axis (fibre-direction axis) of an angle φ. The angle $\varphi = \overline{\varphi}$, which satisfies Equation (8), determines the orientation of the fracture surface. Prior to matrix failure, the angle that maximises the functional part of Equation (8) defines the orientation of the "potential fracture surface" [21] for matrix tensile failure. The tensile strength of a pure polymer resin is strain rate dependent [33]. However, transverse tensile strength is dominated by the strength properties of the weaker fibre/matrix interface, which would greatly depend on the material system and fibre packing arrangement, i.e. not on the solely matrix properties. A quantitative analysis or data reduction of published experimental results for the pure matrix tensile strength is not even possible by virtue of the large scatter [34], [35], [36], [37], [38]. Thus, the matrix tensile failure criterion is formulated with the conservative and simplistic assumption that pure matrix tensile strength is independent of loading-rate.

Off-axis failure properties of UD composites have been investigated in the open literature using compressive [6], [25], [27], [29], [39], [40], or tensile [36] techniques. From these works it can be concluded that both in-plane and interlaminar shear strengths are strongly affected by strain rate. Hence, rate-dependent shear traction strengths $S_{xy}^{d} = k_{x'y'}\left(\dot{\gamma}_{x'y'}\right)S_{xy}^{qs}$ and $S_{yz}^{d} = k_{y'z'}\left(\dot{\gamma}_{y'z'}\right)S_{yz}^{qs}$ are used in the failure criterion for matrix tensile failure.

2.4 Matrix compressive failure

The following criterion is proposed for matrix compressive failure:

$$\begin{cases} \left(\sigma_i\right) \xrightarrow{\perp x(\varphi)} \left(\sigma_{i'}\right) \\ \left(\dot{\varepsilon}_i\right) \xrightarrow{\perp x(\varphi)} \left(\dot{\varepsilon}_{i'}\right) \\ f_{mc} = \left(\dfrac{\tau_{xy'}}{k_{xy'}\left(\dot{\gamma}_{xy'}\right)S_{xy}^{qs} - \mu_l^d \sigma_{y'}}\right)^2 + \left(\dfrac{\tau_{y'z'}}{k_{y'z'}\left(\dot{\gamma}_{y'z'}\right)S_{yz}^{qs} - \mu_t^d \sigma_{y'}}\right)^2 - 1 \geq 0 \end{cases} \quad \text{Equation (9)}$$

Where the symbol $\perp x(\varphi)$ signifies a 3D rotation around the x-axis (fibre-direction axis) of a trial angle $0 \leq \varphi \leq \pi$ [31]. The angle $\varphi = \overline{\varphi}$, which satisfies Equation (9), determines the "fracture plane" orientation. The “master fracture surface”, which defines the boundaries in stress space for the validity of the above criterion, was illustrated in [32]. Prior to matrix failure, the trial angle that maximises the functional part of Equation (9) identifies the orientation of the "potential fracture surface” [21] for matrix compressive failure. The angle φ_0^{qs} identifies the fracture surface orientation for pure transverse QS compressive failure. This angle needs to be measured experimentally and it is typically found that $\varphi_0^{qs} > 50^{\circ}$ for UD polymer matrix composites. The transverse friction coefficient μ_t^{qs} is defined from the Mohr-Coulomb theory as:

$$\mu_t^{qs} = -\frac{1}{\tan\left(2\varphi_0^{qs}\right)}$$ Equation (10)

The angle for dynamic pure transverse compression failure, φ_0^d, is found to be identical to φ_0^{qs} in composites compressed at low, medium and high strain rates, from QS up to a thousand strains per second [30], [41], [42]. Thus, $\mu_t^d = \mu_t^{qs}$ in this regime of strain rates.

The QS longitudinal friction coefficient μ_l^{qs} can be derived using a simple orthotropic model [32]:

$$\mu_l^{qs} = \mu_t^{qs} \frac{S_{xy}^{qs}}{S_{yz}^{qs}}$$ Equation (11)

Where S_{xy}^{qs} is the QS shear strength, and S_{yz}^{qs} is the QS out-of-plane shear strength. The latter is inversely calculated from the transverse compressive strength as:

$$S_{yz}^{qs} = \frac{Y_c^{qs}}{2\tan\left(\varphi_0^{qs}\right)}$$ Equation (12)

However, from Equation (10) and Equation (11), with $\mu_t^d = \mu_t^{qs}$:

$$\mu_l^d = \mu_t^d \frac{S_{xy}^d}{S_{yz}^d} = \mu_t^{qs} \frac{k_{xy}\left(\dot{\gamma}_{xy}\right) S_{xy}^{qs}}{k_{yz}\left(\dot{\gamma}_{yz}\right) S_{yz}^{qs}}$$ Equation (13)

Which is validated using dynamic experimental results [29] – see Figure 4.

Combining Equation (11) and Equation (13) gives:

$$\frac{\mu_l^d}{\mu_l^{qs}} = \frac{S_{xy}^d}{S_{xy}^{qs}} \cdot \frac{S_{yz}^{qs}}{S_{yz}^d} = \frac{k_{xy}\left(\dot{\gamma}_{y'x'}\right)}{k_{yz}\left(\dot{\gamma}_{y'z'}\right)}$$ Equation (14)

Thus, one of the following must also be valid:

$$\begin{cases} I. \quad k_{xy} \neq k_{yz} \Leftrightarrow \mu_l^d \neq \mu_l^{qs} \\ II. \quad k_{xy} = k_{yz} \Leftrightarrow \mu_l^d = \mu_l^{qs} \end{cases}$$ Equation (15)

I.e. either:

I. Longitudinal and transverse shear strengths have different enhancement as a function of loading rate, and the longitudinal friction coefficient μ_l is also affected by loading rate;

or,

II. Longitudinal and transverse shear strengths have an identical enhancement as a function of loading rate and the value of the longitudinal friction coefficient μ_l does not depend on the loading-rate.

Strain rate effects are produced by an isotropic polymer matrix and it seems feasible to assume that both the longitudinal and transverse shear tractions would show similar enhancement with increasing loading rate. This can be proved by using data published in the open literature when calculating the validity of the following equality:

$$k_{xy}\left(\dot{\gamma}_{xy}\right) = k_{yz}\left(\dot{\gamma}_{yz}\right)$$ Equation (16)

Which is derived from Equation (14) with the assumption: $\mu_l = \mu_l^{qs} = \mu_l^d$.

Only a few works are found in the published literature in which both the transverse compressive strength and the longitudinal shear strength of UD polymer composites are characterised[2] at QS and dynamic loading rates [25], [29], [6]. Transverse shear QS strength values are extrapolated from the transverse compression strength data for QS loading rates, using Equation (12) and $\varphi_0^{qs} = 53^\circ$ unless otherwise specified in the original paper. The same method is applied to extrapolate the transverse shear dynamic strength from the transverse compression dynamic strength, using the valid relationship $\varphi_0^d = \varphi_0^{qs}$. Table 2 shows that available published data indicates that longitudinal and transverse shear strengths can be assumed identically affected by strain rate, within experimental scatter. Thus it can be concluded that the longitudinal friction coefficient should also be assumed strain rate independent, over the range of strain rates investigated.

2.5 Summary of the dynamic failure criteria

The validity of Equation (16) has important implications. It is in fact now possible to reformulate the set of the strain rate dependent criteria, Equation (6) plus Equation (7), and Equation (8) plus Equation (9) as follows:

$$f_{fc} = \frac{\sigma_x}{k\left(\dot{\varepsilon}_x^t\right)X_c^{qs}} + \frac{\tau_{xy}}{k\left(\dot{\gamma}_{xy}\right)S_{xy}^{qs}} + \frac{\tau_{zx}}{k\left(\dot{\gamma}_{zx}\right)S_{zx}^{qs}} - 1 \geq 0 \qquad \text{Equation (17)}$$

$$f_{fc} = \frac{\sigma_x}{X_c^{qs}} + \left(\frac{\tau_{xy}}{k\left(\dot{\gamma}_{xy}\right)S_{xy}^{qs}}\right)^{\alpha} + \left(\frac{\tau_{zx}}{k\left(\dot{\gamma}_{zx}\right)S_{zx}^{qs}}\right)^{\alpha} - 1 \geq 0 \qquad \text{Equation (18)}$$

$$f_{mt} = \left(\frac{\sigma_{y'}}{Y_t^{qs}}\right)^2 + \left(\frac{\tau_{xy'}}{k\left(\dot{\gamma}_{xy'}\right)S_{xy}^{qs}}\right)^2 + \left(\frac{\tau_{y'z'}}{k\left(\dot{\gamma}_{y'z'}\right)S_{yz}^{qs}}\right)^2 - 1 \geq 0 \qquad \text{Equation (19)}$$

$$f_{mc} = \left(\frac{\tau_{xy'}}{k\left(\dot{\gamma}_{xy'}\right)S_{xy}^{qs} - \mu_l^d\sigma_{y'}}\right)^2 + \left(\frac{\tau_{y'z'}}{k\left(\dot{\gamma}_{y'z'}\right)S_{yz}^{qs} - \mu_t^d\sigma_{y'}}\right)^2 - 1 \geq 0 \qquad \text{Equation (20)}$$

Equation (17) is applicable for UD composites whose experimental QS failure envelope suggests kink-band development. Equation (18) is applicable for UD composites whose experimental QS failure envelope suggests both shear failure of the fibres or kinking depending on the loading case.

Equations (17)-(20) differ from the earlier Equations (6)-(9) because the new set of criteria is formulated using one solely scaling function, i.e. $k\left(\dot{\varepsilon}_i\right)$, which is characterised with QS and dynamic experimental strength data for one solely mode of deformation, e.g. $\dot{\varepsilon}_4 \equiv \dot{\gamma}_{xy}$.

2.6 The scaling function

[2] The longitudinal dynamic shear strength was not directly characterised in two of these works, but it can be easily extracted from the QS and dynamic failure envelopes, as proposed in [43].

The scaling function $k(\dot{\varepsilon}_i)$, which is the only strain rate dependent parameter required by the dynamic failure criteria, Equations (17)-(20), is calibrated using in-plane shear strength data from QS and dynamic tests. As emphasized by Koerber et al. [28], due to the dependency of the in-plane shear strength on the biaxial stress state, the in-plane shear strength can be determined from the 15˚ and 30˚ off-axis specimens with the extrapolation method proposed by Tsai and Sun [43]. When QS and dynamic shear strength is available, the scaling function $k(\dot{\varepsilon}_i)$ is defined from a polynomial fit of the normalised in-plane shear strength versus shear strain rate values as follows:

$$k(\dot{\gamma}_{xy}) = K_0 + K_1 \log_{10} \dot{\gamma}_{xy} + K_2 \log_{10}^2 \dot{\gamma}_{xy} \qquad \text{Equation (21)}$$

A second order polynomial is typically sufficient as shown in Figure 5, where typical UD carbon/epoxy QS and dynamic data are presented.

3. Numerical implementation: predicting elastic and failure dynamic properties of UD composites with ABAQUS/Explicit

Accurate modelling of the non-linear in-plane shear response is key to achieve accurate modelling of the matrix dominated, 3D elastic and failure dynamic properties. Also, strain-rates can be readily computed from strain increments and time step during an explicit analysis. The relevant equations are presented in this section in incremental form and they can be readily implemented into commercially available software for non-linear FE analysis with an explicit integration scheme, e.g. Abaqus/Explicit, LS-DYNA, etc.

3.1 3D transversely isotropic elastic behaviour and non-linear elastic-plastic shear behaviour

During the explicit analysis, the total strains and stresses are computed at the generic simulation time t in incremental form, for a Δt time step, as follows:

$$\begin{cases} \varepsilon_i^{t+\Delta t} = \varepsilon_i^t + \dot{\varepsilon}_i^{t+\Delta t}\Delta t = \varepsilon_i^t + \Delta\varepsilon_i^{t+\Delta t} \\ \sigma_i^{t+\Delta t} = \sigma_i^t + \dot{\sigma}_i^{t+\Delta t}\Delta t = \sigma_i^t + \Delta\sigma_i^{t+\Delta t} \end{cases} \qquad \text{Equation (22)}$$

Where a vector representation is used for strains and stresses with the following shorthand convention: $i = 1(\equiv x), 2(\equiv y), 3(\equiv z), 4(\equiv xy), 5(\equiv yz), 6(\equiv zx)$. The stress increment vector $\Delta\sigma_i^{t+\Delta t}$ is computed at each time step assuming linear elastic direct behaviour and non-linear (plastic) orthotropic shear stress-strain behaviour as:

$$\begin{bmatrix} \Delta\sigma_x^{t+\Delta t} \\ \Delta\sigma_y^{t+\Delta t} \\ \Delta\sigma_z^{t+\Delta t} \\ \Delta\tau_{xy}^{t+\Delta t} \\ \Delta\tau_{yz}^{t+\Delta t} \\ \Delta\tau_{zx}^{t+\Delta t} \end{bmatrix} = \begin{bmatrix} \frac{1-\nu_{yz}\nu_{zy}}{E_y E_z \mathrm{A}} & \frac{\nu_{yx}+\nu_{zx}\nu_{yz}}{E_y E_z \mathrm{A}} & \frac{\nu_{zx}+\nu_{yx}\nu_{zy}}{E_y E_z \mathrm{A}} & 0 & 0 & 0 \\ \frac{\nu_{xy}+\nu_{xz}\nu_{zy}}{E_x E_z \mathrm{A}} & \frac{1-\nu_{zx}\nu_{xz}}{E_x E_z \mathrm{A}} & \frac{\nu_{zy}+\nu_{zx}\nu_{xy}}{E_x E_z \mathrm{A}} & 0 & 0 & 0 \\ \frac{\nu_{xz}+\nu_{xy}\nu_{yz}}{E_y E_x \mathrm{A}} & \frac{\nu_{yz}+\nu_{xz}\nu_{yx}}{E_y E_x \mathrm{A}} & \frac{1-\nu_{xy}\nu_{yx}}{E_y E_x \mathrm{A}} & 0 & 0 & 0 \\ 0 & 0 & 0 & \overline{G}_{xy} & 0 & 0 \\ 0 & 0 & 0 & 0 & \overline{G}_{yz} & 0 \\ 0 & 0 & 0 & 0 & 0 & \overline{G}_{zx} \end{bmatrix} \begin{bmatrix} \Delta\varepsilon_x^{t+\Delta t} \\ \Delta\varepsilon_y^{t+\Delta t} \\ \Delta\varepsilon_z^{t+\Delta t} \\ \Delta\gamma_{xy}^{t+\Delta t} \\ \Delta\gamma_{yz}^{t+\Delta t} \\ \Delta\gamma_{zx}^{t+\Delta t} \end{bmatrix} \qquad \text{Equation (23)}$$

With,

$$\mathrm{A} = \frac{1-\nu_{xy}\nu_{yx}-\nu_{yz}\nu_{zy}-\nu_{zx}\nu_{xz}-2\nu_{xy}\nu_{yz}\nu_{zx}}{E_x E_y E_z} \qquad \text{Equation (24)}$$

And where $\gamma_i = 2\varepsilon_i$ are the engineering shear strains, with $i \geq 4$.

The direct behaviour is assumed transversely isotropic, i.e. $E_y = E_z$, and $\nu_{yz} = \nu_{zy}$. The tangent shear moduli $\overline{G}_i$, are defined as:

$$\overline{G}_i^{t+\Delta t} = \sum_{k=1}^{4} G_{i,k}\left(\gamma_i^{t+\Delta t}\right)^k, i \geq 4 \qquad \text{Equation (25)}$$

The four coefficients $G_{i,k}$ need to be determined from polynomial fit of the experimental data for the $\tau_{xy}(\gamma_{xy}), \tau_{yz}(\gamma_{yz})$ and $\tau_{zx}(\gamma_{zx})$ behaviours. A maximum shear strain up to which the polynomial fits are valid, $\gamma_{P,\max}$, is user defined:

$$\begin{cases} \gamma_{xy}^{t+\Delta t} > \gamma_{P,\max} \rightarrow \overline{G}_{xy}^{t+\Delta t} = hG_{xy,0} \\ \gamma_{yz}^{t+\Delta t} > \gamma_{P,\max} \rightarrow \overline{G}_{yz}^{t+\Delta t} = \overline{G}_{yz}\left(\gamma_{P,\max}\right) \\ \gamma_{zx}^{t+\Delta t} > \gamma_{P,\max} \rightarrow \overline{G}_{zx}^{t+\Delta t} = hG_{zx,0} \end{cases} \qquad \text{Equation (26)}$$

Where for $\gamma_{xy}^{t+\Delta t} > \gamma_{P,\max}$ the tangent in-plane and out-of-plane shear stiffness are user defined through the parameter h to improve the correlation between the curve fit and the test results at large shear strains. The model assumes that the material unloads in shear with initial shear stiffness $G_{i,1}$ and that inelastic strain is recovered upon complete unloading from inelastic states with zero associated stress.

3.2 Modelling strain-rate induced material hardening

Strain-rate induced hardening in metals can be explained by the theory of dislocations, whose motion and slipping is also governed by shear forces at the lattice scale, e.g. [44]. When the (shear) loading rate increases and overcomes the rate of recovery, more dislocations are generated and entangle, which is the reason for strain rate material hardening experimentally observed for these materials. A similar interpretation is typically given for polymers: their micro-structure is composed of molecular chains which flow with deformation [45], and thus can entangle if the deformation rate exceeds the rate of recovery.

Based on these phenomenological observations, it could be argued that, for carbon fibre polymer composites, the solely mode of deformation that is strain rate sensitive is the matrix shear mode, and that strain rate effects on both strength and stiffness in modes other than shear are a 3D effect, due to the fact that the planes of maximum shear stress are at an angle to the principal planes of material symmetry.

Strain rate would affect “progressive failure”, thus plastic flow and matrix cracking in polymers and polymer composites. These effects are typically not distinguished in current macro-mechanical theories and are here referred to in a general manner as “strain rate effects”. Within this context, a distinction is made between the physical concept of “fracture surface”, which has originally been used in [31], and the physical concept of “surface of progressive failure”, which is here introduced to simulate resistance to progressive failure observed in composites subjected

to higher rate loading conditions. The "potential fracture surface" can be used to define the orientation of this plane, on which progressive failure, i.e. visco-plasticity effects when the focus is on strain rate effects, accumulates in a composite volume under generic loading conditions. This orientation, i.e. $\overline{\varphi}$, is defined using the functional part of the matrix compressive failure criterion as follows[3]:

$$\begin{cases} f_{mc}^{t+\Delta t}(\varphi)=\left(\dfrac{\tau_{xy'}^{t+\Delta t}(\varphi)}{k\left(\dot{\gamma}_{xy'}(\varphi)\right)S_{xy}^{qs}-\mu_l^{qs}\sigma_{y'}^{t+\Delta t}(\varphi)}\right)^2+\left(\dfrac{\tau_{y'z'}^{t+\Delta t}(\varphi)}{k\left(\dot{\gamma}_{y'z'}(\varphi)\right)S_{yz}^{qs}-\mu_t^{qs}\sigma_{y'}^{t+\Delta t}(\varphi)}\right)^2 \\ \overline{\varphi}: f_{mc}^{t+\Delta t}(\overline{\varphi})> f_{mc}^{t+\Delta t}(\varphi)\forall\varphi\in[0,2\pi[\end{cases} \quad \text{Equation (27)}$$

However, Equation (27) does not predict whether plasticity has or has not yet initiated, and visco-plasticity effects (hardening) can be predicted only when further data is available. Based on the phenomenological interpretation proposed in this work, the required information is obtained from pure shear loading data. The shear stress-strain curves of composites are typically non-linear, strain rate dependent curves. Their slopes provide implicit information on whether visco-plasticity has initiated at a given shear strain and the effects of this on the shear meso-mechanical properties.

Thus, strain-rate induced hardening can be predicted by modelling strain rate dependent shear stress-strain response on the "progressive failure plane", whose orientation is predicted by application of Equation (27).

In Section 2.4 it was proposed that, for transversely isotropic continuous fibrous composites, the effects of strain rate on the transverse (longitudinal) shear stress-strain behaviour in the rotated potential fracture plane can be assumed independent of the rotation angle. In this same Section 2.4 it was also proved that the dynamic effects on the transverse shear stress-strain response in the plane of progressive failure are identical to those observed in in-plane shear experiments. Thus, the proposed approach for the 3D modelling of strain rate material hardening in UD polymer composites is the following:

$$\begin{bmatrix}\Delta\varepsilon_x^{t+\Delta t}\\ \Delta\varepsilon_y^{t+\Delta t}\\ \Delta\varepsilon_z^{t+\Delta t}\\ \Delta\gamma_{xy}^{t+\Delta t}\\ \Delta\gamma_{yz}^{t+\Delta t}\\ \Delta\gamma_{zx}^{t+\Delta t}\end{bmatrix}\xrightarrow{\perp x(\overline{\varphi})}\begin{bmatrix}\Delta\varepsilon_x^{t+\Delta t}\\ \Delta\varepsilon_{y'}^{t+\Delta t}\\ \Delta\varepsilon_{z'}^{t+\Delta t}\\ \Delta\gamma_{xy'}^{t+\Delta t}\\ \Delta\gamma_{y'z'}^{t+\Delta t}\\ \Delta\gamma_{z'x}^{t+\Delta t}\end{bmatrix}\Rightarrow\begin{Bmatrix}k\left(\dot{\varepsilon}_x^{t+\Delta t}\right)\\ k\left(\dot{\gamma}_{xy'}^{t+\Delta t}\right)\\ k\left(\dot{\gamma}_{y'z'}^{t+\Delta t}\right)\\ k\left(\dot{\gamma}_{z'x}^{t+\Delta t}\right)\end{Bmatrix}$$

$$\begin{bmatrix}\Delta\sigma_x^{t+\Delta t}\\ \Delta\sigma_y^{t+\Delta t}\\ \Delta\sigma_z^{t+\Delta t}\\ \Delta\tau_{xy}^{t+\Delta t}\\ \Delta\tau_{yz}^{t+\Delta t}\\ \Delta\tau_{zx}^{t+\Delta t}\end{bmatrix}\xrightarrow{\perp x(\overline{\varphi})}\begin{bmatrix}\Delta\sigma_x^{t+\Delta t}\\ \Delta\sigma_{y'}^{t+\Delta t}\\ \Delta\sigma_{z'}^{t+\Delta t}\\ \Delta\tau_{xy'}^{t+\Delta t}\\ \Delta\tau_{y'z'}^{t+\Delta t}\\ \Delta\tau_{z'x}^{t+\Delta t}\end{bmatrix}\Rightarrow\begin{bmatrix}\Delta\sigma_x^{t+\Delta t}\\ \Delta\sigma_{y'}^{t+\Delta t}\\ \Delta\sigma_{z'}^{t+\Delta t}\\ k\left(\dot{\gamma}_{xy'}^{t+\Delta t}\right)\Delta\tau_{xy'}^{t+\Delta t}\\ k\left(\dot{\gamma}_{y'z'}^{t+\Delta t}\right)\Delta\tau_{y'z'}^{t+\Delta t}\\ k\left(\dot{\gamma}_{z'x}^{t+\Delta t}\right)\Delta\tau_{z'x}^{t+\Delta t}\end{bmatrix}\xrightarrow{\perp x(-\overline{\varphi})}\begin{bmatrix}\Delta\sigma_x^{t+\Delta t}\\ \Delta\sigma_y^{t+\Delta t}\\ \Delta\sigma_z^{t+\Delta t}\\ \Delta\tau_{xy}^{t+\Delta t}\\ \Delta\tau_{yz}^{t+\Delta t}\\ \Delta\tau_{zx}^{t+\Delta t}\end{bmatrix}^{dyn} \quad \text{Equation (28)}$$

[3] the theory is formulated and validated for combined compression/shear loading conditions, but the combined tensile/shear loading cases are similarly treated following application of the criterion Equation (19), which is also based on application of the potential fracture surface concept.

Where the symbol $\perp x(\varphi)$ signifies a 3D rotation around the x-axis (fibre-direction axis) of the angle $\overline{\varphi}$, which is defined in Equation (27) and $\Delta\left(\sigma_i^{t+\Delta t}\right)^{dyn}$ is the dynamic stress increments vector, which is used in the explicit stress-update procedure, Equation (22).

4. Validation

The failure criteria and the approach for predicting strain rate induced material hardening are implemented in ABAQUS/Explicit for one-integration point solid elements. The overall approach is validated against the experimental results of Koerber et al. [28], [29]. They tested an IM7-8552 UD composite under QS and dynamic off-axis and longitudinal compression using a Hopkinson bar, pulse shape technique and digital image correlation at the higher strain rates of ~300/s^{-1}. They also published the full set of axial stress-strain data, against which it is possible to test the predictive capabilities of the proposed modelling approach.

Here, the criterion in Equation (17) is chosen because the IM7-8552 UD composite showed to fail by fibre kinking at QS rates [29].

One single element simulations are performed with the following material input properties, which are all directly extracted from the available experimental results [28], [29]:

$E_x = 165000MPa$; $E_y = E_z = 7700MPa$; $\nu_{xy} = \nu_{zx} = 0.3$; $\nu_{yz} = 0.3$;

$G_{xy,1} = G_{zx,1} = 5643MPa$; $G_{xy,2} = G_{zx,2} = -108606.81MPa$;

$G_{xy,3} = G_{zx,3} = 940510.37MPa$; $G_{xy,4} = G_{zx,4} = -2932104.6MPa$; $G_{yz,1} = 4000MPa$;

$G_{yz,2} = G_{yz,3} = G_{yz,4} = 0$; $\gamma_{P,\max} = 0.07$, $h = 0.05$; $K_0 = 1.2626$; $K_1 = 0.0656$; $K_2 = 0$

$\varphi_0 = 52^\circ$; $X_c^{QS} = 1023MPa$; $Y_c^{QS} = 255MPa$; $S_{xy}^{QS} = S_{zx}^{QS} = 100MPa$.

Figure 6 shows a comparison between the experimental [29] and the numerical in-plane shear QS behaviours. This Figure 6 illustrates the validity for the extracted values of the fitting parameters, $G_{xy,k}$, and of the parameters $\gamma_{P,\max}$ and h.

Figure 7 shows a comparison between the experimental and the numerical in-plane dynamic shear behaviours. This Figure 7 illustrates the validity of the extracted K_i constants of the rate-dependent function k. The stress-strain curves in Figure 7 have been truncated at a value of in-plane shear strength extrapolated from the 15˚ and 30˚ off-axis data, as discussed in Section 2.4.

One-solid element numerical simulations are conducted for longitudinal compressive QS and dynamic loadings conditions, and results are presented in Figure 8. Simulations are then carried out for the full range of off-axis and transverse compression specimen configurations investigated in [29], and a comparison between experimental and numerical axial stress-strain results is presented in Figure 9.

5. Discussion

The numerical curves in Figure 8 and Figure 9 are truncated at the predicted value of failure stress, which shows that the implemented failure criteria can predict strength values for all off-axis, transverse and longitudinal compressive cases, which are in excellent agreement with the experimental results, for both QS and dynamic loading conditions. Strain rate induced material hardening effects are also excellently captured at the higher loading rate. The moduli are

predicted very accurately for all dynamic cases. This validates the use of a same strain rate dependent scaling function for both strength and moduli, on the potential surface for progressive failure, at least for the IM7-8552 UD composite material here investigated.

The experimental curves in Figure 9 show non-linear stress-strain behaviour at higher off-axis angles and for transverse compression. This is not captured in the simulations because non-linear material response is modelled only for the in-plane and out-of-plane shear behaviours in the present work, and not for the direct behaviour. The development of a suitable approach for phenomenological-based modelling of direct non-linear stress-strain behaviour should be addressed by future research. This could be formulated using a definition of plastic strain based on an equivalent shear strain defined on the plane of progressive failure, similarly to what originally proposed in [46].

The applicability of the proposed approach is validated for combined compressive/shear loading conditions, but it should be assessed also for off-axis tensile loading conditions. This has not been attempted here for the lack of detailed experimental results in the literature. Off-axis tensile dynamic tests results should be generated because a different strain rate sensitivity of the composite compared to the compressive case might be expected due to a combined effect of hydrostatic pressure and strain rate, which has been observed experimentally [26].

Finally, it is noted that based on the excellent agreement achieved for strength and moduli for all off-axis configurations, the scaling function k, which has been here extracted from in-plane shear strength data, could have also been extracted with an inverse approach using data generated from any other off-axis angle, or from the pure transverse compression strength data, or even from the QS and dynamic longitudinal compression strength data.

6. Conclusions

Predicting the dynamic behaviour of UD polymer composites is a difficult task because of their strongly anisotropic elastic and failure behaviour. Also, characterisation of their dynamic behaviour requires application of complex, time-consuming and non-standard experimental techniques.

Classic approaches based on visco-plasticity formulations, and currently available dynamic failure theories, typically require calibration using either dynamic tests data for many different specimen configurations, i.e. off-axis dynamic compression at many different angles, or micro-mechanical simulations.

This paper has proposed a novel macro-mechanical approach for the FE modelling of 3D strain rate effects in UD carbon fibre polymer composites, which is based on phenomenological sound arguments.

It has been shown that the off-axis compressive dynamic behaviour of UD carbon fibre polymer composites can be fully predicted, i.e. moduli and strength, when data is produced from a very limited number of QS and dynamic tests for one solely specimen configuration. This is a dramatic improvement compared to what is required for applicability of other currently available modelling techniques. The key to achieve this was to postulate that, for carbon fibre polymer composites, the solely mode of deformation that is strain rate sensitive is the matrix shear mode, and that strain rate effects on both strength and stiffness in modes other than shear are a 3D effect, due to the fact that the planes of maximum shear stress are at an angle to the principal planes of material symmetry.

The proposed approach is easy to implement in FE, and it is shown to predict material behaviour in an uncharacterised dynamic loading space with great accuracy. Thus, it can not only be applied for virtual design of composite structures subjected to dynamic high-rate loading conditions, but also for virtual dynamic characterisation of UD carbon fibre composite materials.

It is noted that the shear and direct behaviours are fully decoupled in the proposed approach. Thus, a method for predicting the dynamic behaviour of UD composites with strain rate dependent fibre properties, such as glass or high performance fibre composites, can be seen as the natural extension of the current approach, where direct strain rate dependent material behaviour is also included for the modelling of strain rate dependent fibre properties. This will be the object of future research.

Future research should also clarify the effects of compressive loading (hydrostatic pressure) on the characterised strain rate dependent behaviour and scaling function. This could be achieved by experimental characterisation of both the tensile and the compressive off-axis dynamic behaviours.

Finally, the proposed approach could be further modified to include the modelling of material non-linear behaviour for direct matrix dominated modes of deformation. This could also use phenomenological-based arguments and the concept of “plane of progressive failure” described in this paper.

Acknowledgments

The authors would like to gratefully acknowledge the funding from the Engineering ad Physical Sciences Research Council (EPSRC) and the Defence Science and Technology Laboratory (DSLT) for this research under the project “Improving Survivability of Structures to Impact and Blast Loadings”, EPSRC Reference: EP/G042861/1.

References

[1]. Weeks, CA and Sun, CT. *Modeling non-linear rate-dependent behavior in fiber-reinforced composites.* Compos Sci Technol, Vol. 58, pp. 603-11, 1998.
[2]. Thiruppukuzhi, SV and Sun, CT. *Models for the strain rate dependent behaviour of polymer composites.* Compos Sci Technol, Vol. 61, pp. 1-12, 2001.
[3]. Espinosa, HD, Lu, HC, Zavattieri, PD, Dwivedi, S. *A 3-D Finite Deformation Anisotropic Visco-Plasticity Model for Fiber Composites.* J Compos Mat, Vol. 35, pp. 369-410, 2001.
[4]. Goldberg, RK and Stouffer, DC. *Strain Rate Dependent Analysis of a Polymer Matrix Composite Utilizing a Micromechanics Approach.* J Compos Mater, Vol. 36, pp. 773-94, 2002.
[5]. Tabiei, A and Aminjikarai, SB. *A strain-rate dependent micro-mechanical model with progressive post-failure behavior for predicting impact response of unidirectional composite laminates.* Compos Struct, Vol. 88, pp. 65-82, 2009.
[6]. Daniel, IM, Werner, BT and Fenner, JS. *Strain-rate-dependent failure criteria for composites.* Compos Sci Technol, Vol. 71, pp. 357-364, 2010.
[7]. Barre, S, Chotard, T and Benzeggagh, ML. *Comparative study of strain rate effects on mechanical properties of glass fibre-reinforced thermoset matrix composite.* Compos, Part A: Appl Sci Manuf, Vol. 27, pp. 1169-82, 1996.
[8]. Harding, J and Welsh, LM. *A tensile tensting technique for fibre-reinforced composites at impact rates of strain.* J Mater Sci, Vol. 18, pp. 1810-26, 1983.
[9]. Zhou, Y, Jiang, D and Xia, Y. *Tensile mechanical behavior of T300 and M40J fiber bundles at different strain rate.* J Mater Sci, Vol. 36, pp. 919-22, 2001.
[10]. Gutkin, R, Pinho, ST, Robinson, P, Curtis, PT. *On the transition from shear-driven fibre compressive failure to fibre kinking in notched CFRP laminates under longitudinal compression.* Compos Sci Technol, Vol. 70, pp. 1223-31, 2010.
[11]. Gutkin, R, Pinho, ST, Robinson, P, Curtis, PT. *Micro-mechanical modelling of shear-driven fibre compressive failure and of fibre kinking for failure envelope generation in CFRP.* Compos Sci Technol, Vol. 70, pp. 1214-22, 2010.
[12]. Jelf, PM and Fleck, NA. *The failure of composite tubes due to combined compression and torsion.* J Mater Sci, Vol. 29, pp. 3080-4, 1994.
[13]. Soden, P, Hinton, M and Kaddour, A. *Biaxial test results for strength and deformation of a range of e-glass and carbon fibre reinforced composite laminates: failure exercise benchmark data.* Compos Sci Technol, Vol. 62, pp. 1489-514, 2002.
[14]. Michaeli, W, Mannigel, M and Preller, F. *On the effect of shear stresses on the fibre failure behaviour in cfrp.* Compos Sci Technol, Vol. 69, pp. 1354-7, 2009.
[15]. Gol'demblat, II and Kopnov, VA. *Criteria of Strength and Ductility of Structural Materials [in Russian].* Moscow, 1968.
[16]. Tsai, SW and Wu, EM. *A general theory of strength for anisotropic materials.* J Compos Mater, Vol. 5, pp. 58-80, 1971.
[17]. Hashin, Z. *Failure Criteria for Unidirectional Fiber Composites.* J Appl Mech, Vol. 47, pp. 329-34, 1980.
[18]. Argon, AS. Fracture in composites. *Treatise on Materials Science and Technology.* New York, Academic Press, 1972, pp. 79-114.
[19]. Budiansky, B. *Micromechanics.* Computers and Structures, Vol. 16, pp. 3-12, 1983.
[20]. Davila, CG, Camanho, PP and Rose, CA. *Failure criteria for FRP Laminates.* J Compos Mater, Vol. 39, pp. 323-45, 2005.
[21]. Pinho, ST, Iannucci, L and Robinson, P. *Physically-based failure models and criteria for laminated fibre-reinforced composites with emphasis on fibre kinking: Part I: Development.* Compos, Part A: Appl Sci Manuf, Vol. 37, pp. 63-73, 2006.
[22]. Li, Z and Lambros, J. *Determination of the dynamic response of brittle composites by the use of the split Hopkinson pressure bar.* Compos Sci Technol, Vol. 59, pp. 1097-107, 1999.
[23]. Woldesenbet, E and Vinson, JR. *Specimen Geometry Effects on High-Strain-Rate Testing of Graphite/Epoxy Composites.* AIAA J, Vol. 37, pp. 1102-6, 1999.
[24]. Woldesenbet, E, Gupta, N and Vinson, JR. *Determination of moisture effects on impact properties of composite materials.* J Mater Sci, Vol. 37, pp. 2693-8, 2002.

[25]. Hsiao, HM and Daniel, IM. *Strain rate behavior of composite materials.* Compos Part B-Eng, Vol. 29, pp. 521-34, 1998.
[26]. Pae, KD and Carlson, KS. *The Combined Effects of Hydrostatic Pressure and Strain-Rate on the Compressive Properties of a Laminated, Multi-Directional, Graphite/Epoxy Thick-Composite.* J Compos Mater, Vol. 32, pp. 49-67, 1998.
[27]. Hsiao, HM, Daniel, IM and Cordes, RD. *Dynamic Compressive Behaviour of Thick Composite Materials.* Exp Mech, Vol. 38, pp. 172-80, 1998.
[28]. Koerber, H and Camanho, PP. *High strain rate characterisation of unidirectional carbon–epoxy IM7-8552 in longitudinal compression.* Compos, Part A: Appl Sci Manuf, Vol. 42, pp. 462-70, 2011.
[29]. Koerber, H, Xavier, J and Camanho, PP. *High strain rate characterisation of unidirectional carbon-epoxy IM7-8552 in transverse compression and in-plane shear using digital image correlation.* Mech Mat, Vol. 42, pp. 1004-19, 2010.
[30]. Wiegand, J. *Constitutive modelling of composite materials under impact loading.* PhD Thesis, University of Oxford, Department of Engineering Science. 2008.
[31]. Puck, A. *Puck, Festigkeitsanalyse von Faser-Matrix-Laminaten.* Munich, Hanser, 1996.
[32]. Puck, A and Schurmann, H. *Failure analysis of FRP laminates by means of physically based phenomenological models.* Compos Sci Technol, Vol. 58, pp. 1045-67, 1998.
[33]. Gerlach, R, Siviour, CR, Petrinic, N, Wiegand, J. *Experimental haracterisation and constitutive modelling of RTM-6 resin under impact loading.* Polymer, Vol. 49, pp. 2728-37, 2008.
[34]. *High velocity impact of composite aircraft structures.* 2000. DG XXII Industrial and Materials Technologies Programme. HICAS Contract No. BRPR-CT97-0543.
[35]. Lowe, A. *Matrix-dominated tensile behaviour of unidirectional T300/914 and structural modelling of the material.* J Mater Sci, Vol. 31, pp. 983-93, 1996.
[36]. Gilat, A, Goldberg, RK and Roberts, GD. *Experimental study of strain-rate-dependent behavior of carbon/epoxy composite.* Compos Sci Technol, Vol. 62, pp. 1469-76, 2002.
[37]. Gomez-del Rio, T, Barbero, E, Zaera, R, Navarro, C. *Dynamic tensile behaviour at low temperature of CFRP using a split Hopkinson pressure bar.* Compos Sci Technol, Vol. 65, pp. 61-71, 2005.
[38]. Daniel, IM, Hamilton, WG and La Bedz, RH. Strain characterisation of unidirectional graphite/epoxy composite. Composite materials: Testing and design (sixth conference). Philadelphia : ASTM, 1982. ASTM STP 787.
[39]. Jadhav, A, Woldesenbet, E and Pang, SS. *High strain rate properties of balanced angle-ply graphite/epoxy composites.* Compos Part B-Eng, Vol. 34, pp. 339-46, 2003.
[40]. Vinson, JR and Woldesenbet, E. *Fiber Orientation Effects on High Strain Rate Fiber Orientation Effects on High Strain Rate.* J Compos Mater, Vol. 35, pp. 509-21, 2001.
[41]. Kawai, M and Saito, S. *Off-axis strength differential effects in unidirectional carbon/epoxy laminates at different strain rates and predictions of associated failure envelopes.* Compos Part A-App S, Vol. 40, pp. 1632-49, 2009.
[42]. Vural, M and Ravichandran, G. *Transverse Failure in Thick S2-Glass/ Epoxy Fiber-Reinforced Composites.* J Compos Mater, Vol. 38, pp. 609-23, 2004.
[43]. Tsai, JL and Sun, CT. *Strain rate effect on in-plane shear strength of unidirectional polymeric composites.* Compos Sci Technol, pp. 1941-7, 2005.
[44]. Smoluchowsky, R. *Dislocation in Solids.* New York : John Wiley and Sons, 1957.
[45]. Ward, IM. *Mechanical properties of solid polymers.* New York : John Wiley and Sons, 1982.
[46]. Raimondo, L. *Predicting the dynamic behaviour of polymer composites.* Aeronautics, Imperial College London. London : s.n., 2007. Ph.D. Thesis.

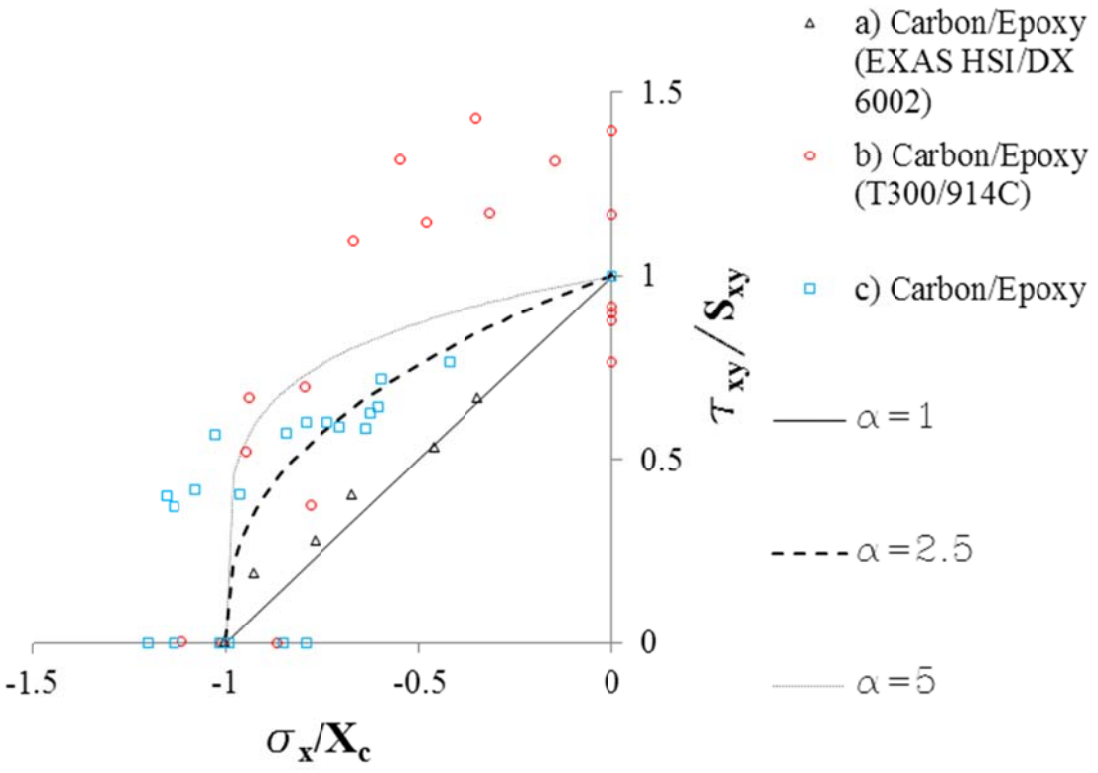

Figure 1. Failure envelopes for combined longitudinal compression/in-plane shear QS loading conditions: a) Jelf and Fleck [12], b) Soden et al. [13] and c) Michaeli et al. [14].

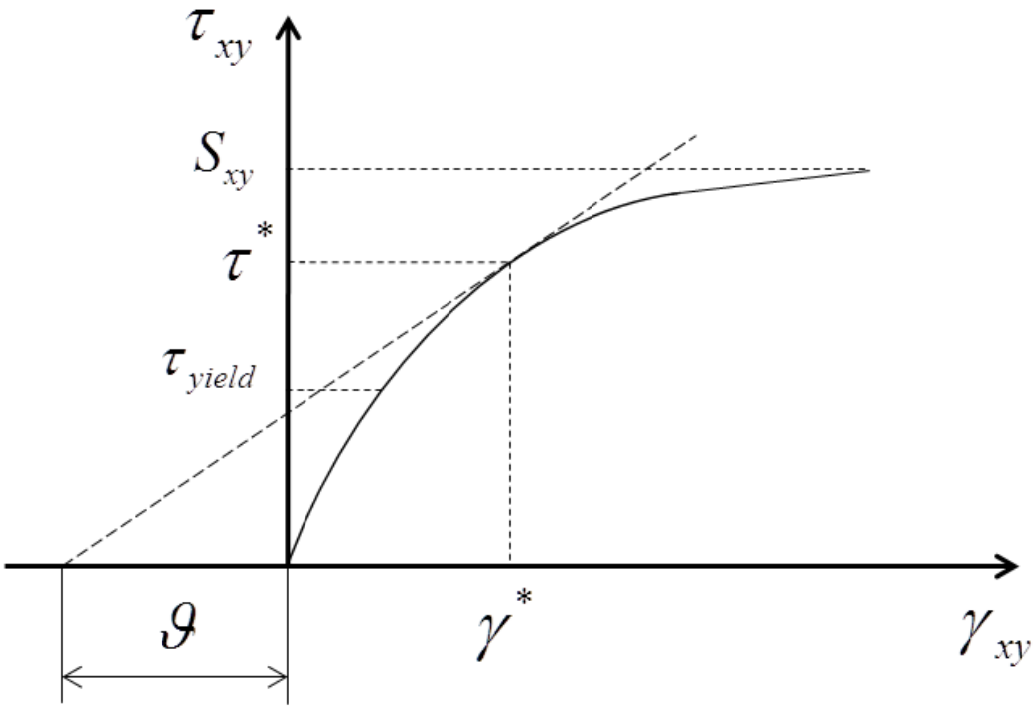

Figure 2. Graphical determination of longitudinal compressive strength based on Equation (3) [25].

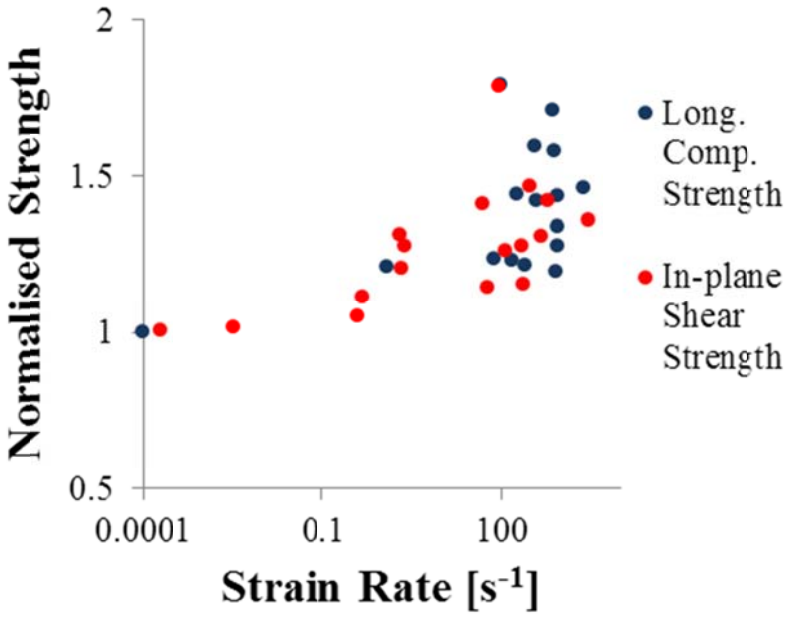

Figure 3. Experimental normalised longitudinal compressive and in-plane shear strength versus strain rate from various sources in the literature as collated in [30].

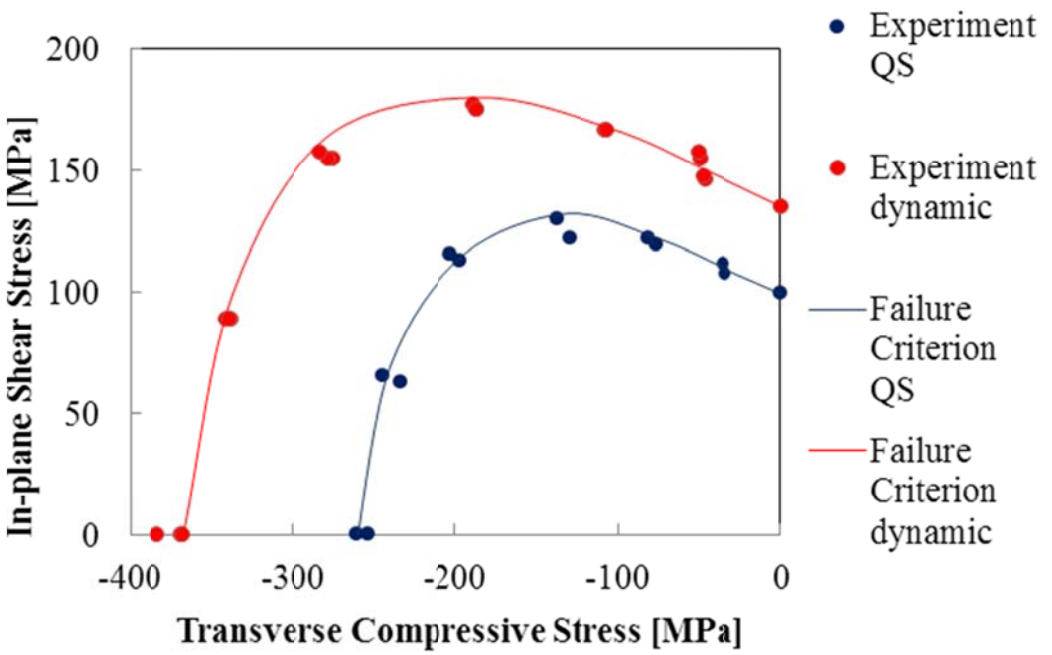

Figure 4. QS and dynamic experimental [29] and theoretical (Equation (9)) failure envelopes for combined transverse compression/in-plane shear for UD carbon-epoxy IM7-8552 composite.

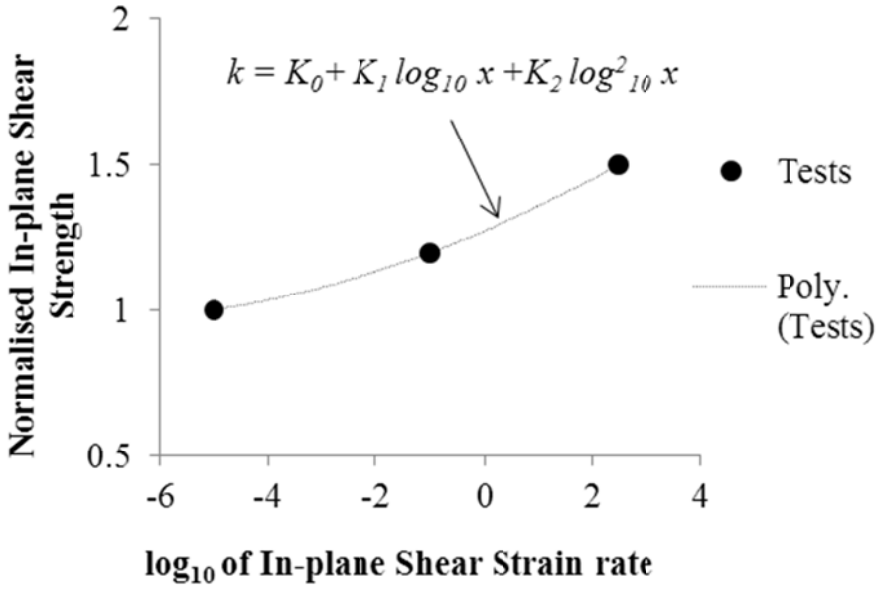

Figure 5. Calibration of the scaling function k using in-plane shear strength data. The tests data is from Hsiao and Daniel [25].

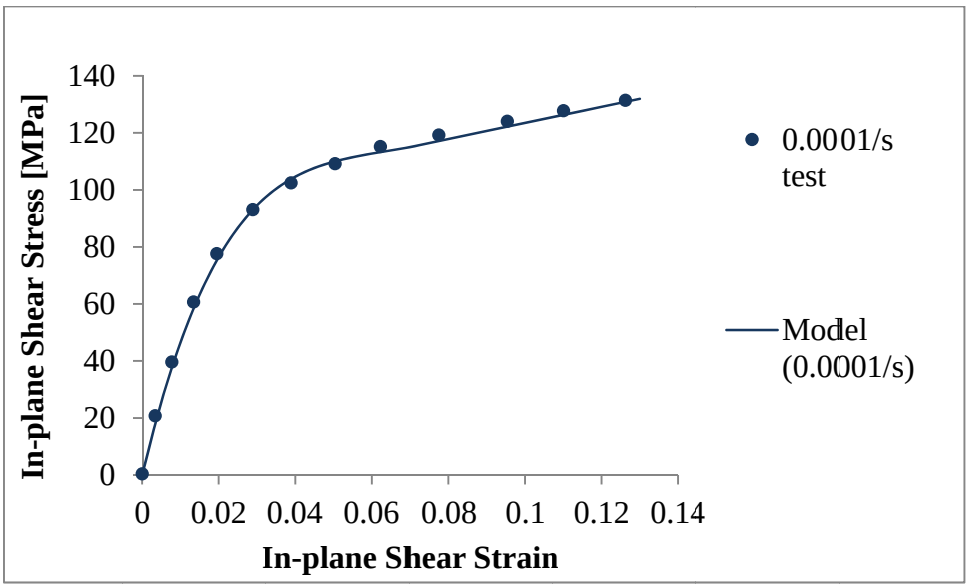

Figure 6. Numerical and experimental [29] QS in-plane shear stress-strain behaviour for an IM7-8552 UD composite.

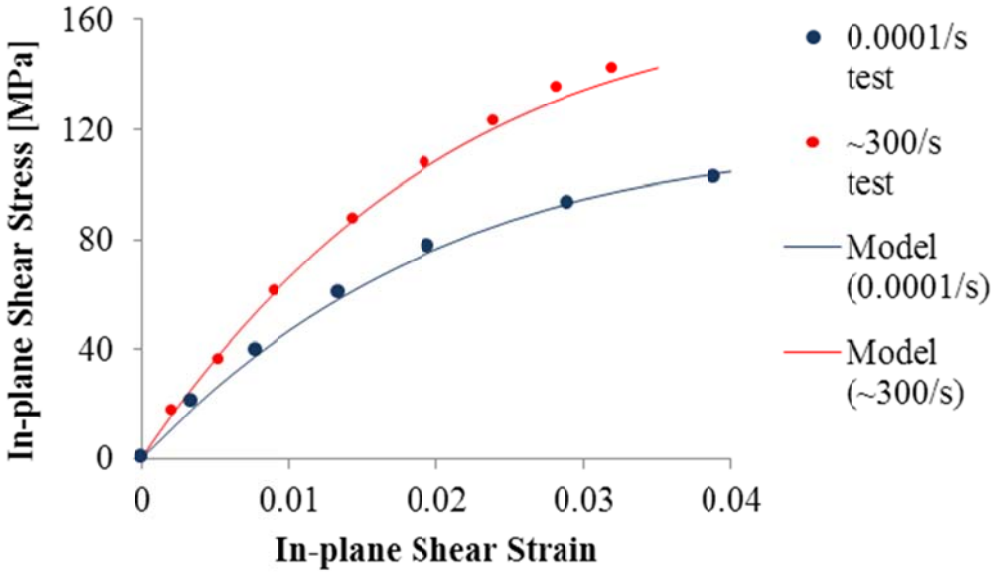

Figure 7. Numerical and experimental [29] QS and dynamic in-plane shear stress-strain behaviour for an IM7-8552 UD composite.

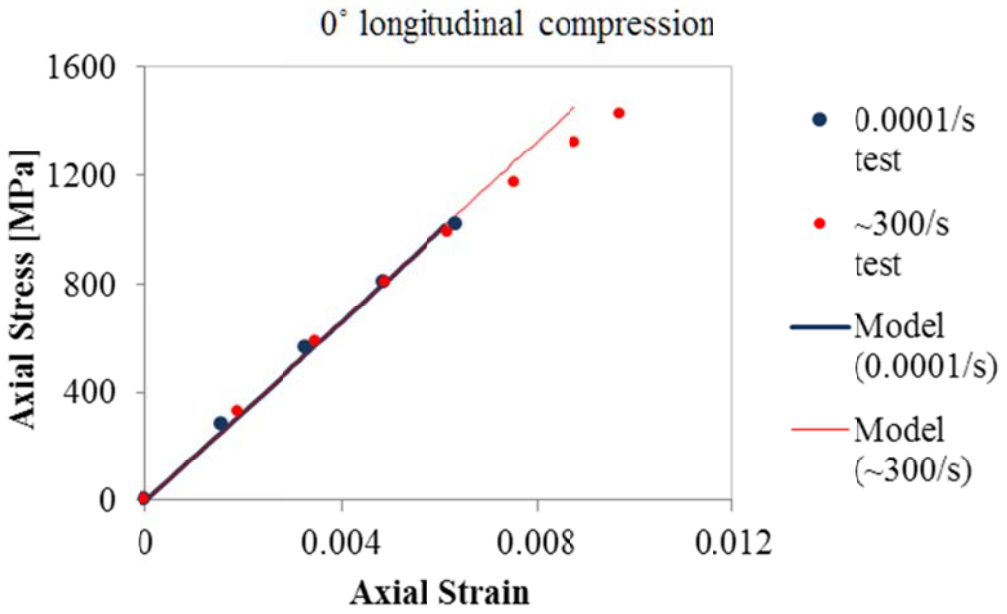

Figure 8. Numerical and experimental [28] longitudinal QS and dynamic stress-strain behaviour of an IM7-8552 UD composite.

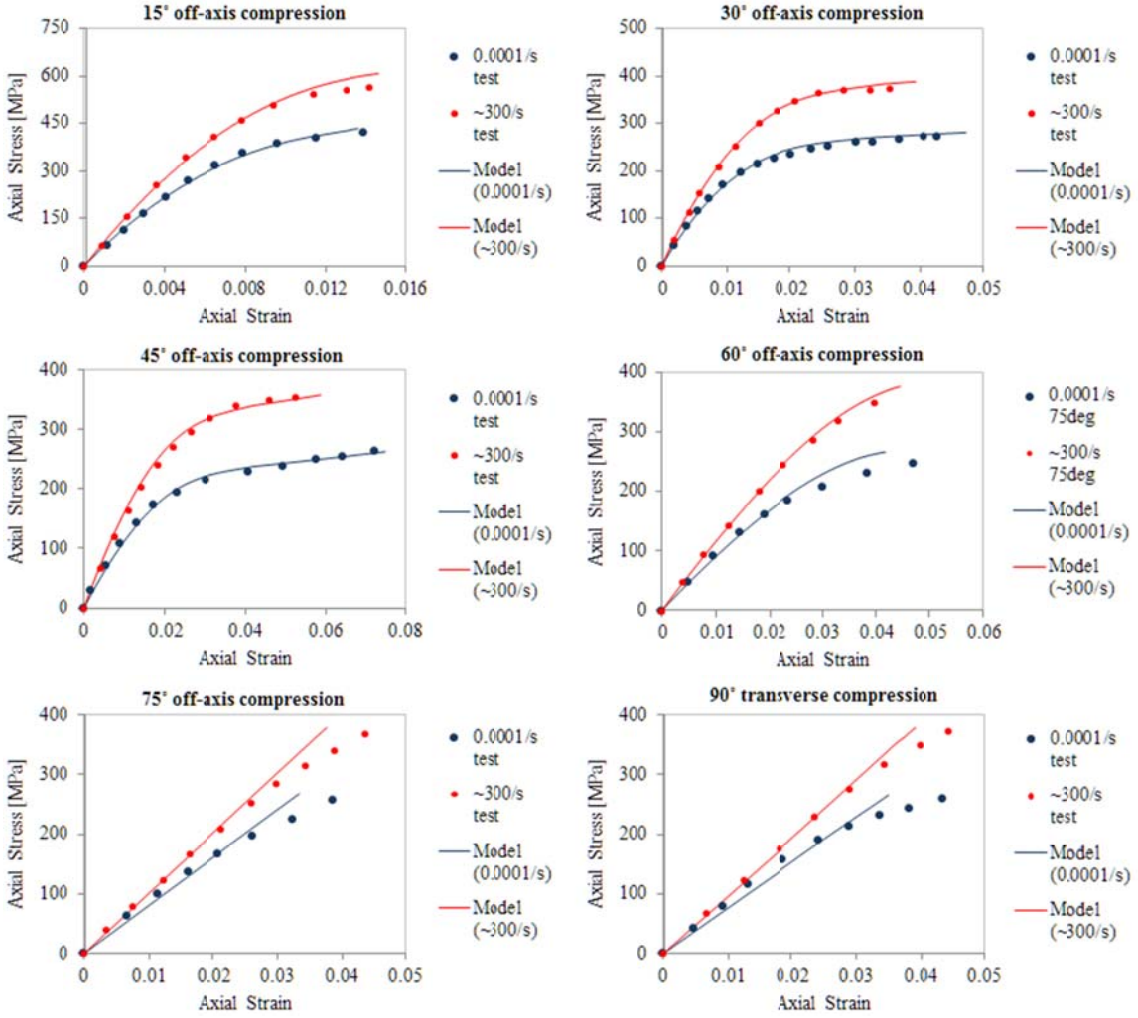

Figure 9. Numerical and experimental [29] QS and dynamic off-axis compressive behaviour of an IM7-8552 UD composite.

Table 1. Validity check for Equation (4)

Material	X_c^{qs} (test)	X_c^{d} (test)	X_c^{d} (Equation (4))	Strain Rates
IM6G/3501-6 [25]	797 MPa	1238 MPa	1162 MPa	$10^{-4} – 10^{2}$ s^{-1}
IM7-8552 [28]	1023 MPa	1417 MPa	1405 MPa	$10^{-4} – 10^{2}$ s^{-1}

Table 2. Validity check for Equation (16)

Material	Percentage error in Equation (16)	Strain rates
IM6G/3501-6 [25]	1.8%	$10^{-4} – 300$ s^{-1}
IM7-8552 [29]	5.3%	$10^{-4} – 350$ s^{-1}
AS4/3501-6 [6]	0.48%	$10^{-4} – 400$ s^{-1}